ELSEVIER

Journal of Physics and Chemistry of Solids 63 (2002) 719–724

JOURNAL OF PHYSICS AND CHEMISTRY OF SOLIDS

www.elsevier.com/locate/jpcs

XAFS at Eu–L_3 edge and UV–VUV excited luminescence of europium doped strontium borophosphate prepared in air

H.-B. Liang[a], Q. Su[a,b,*], Y. Tao[c], T.-D. Hu[c], T. Liu[c], S.L.E. Shulin[d]

[a]*Laboratory of Rare Earth Chemistry and Physics, Changchun Institute of Applied Chemistry, Chinese Academy of Sciences, Changchun, Jilin 130022, China*

[b]*School of Chemistry and Chemical Engineering, Zhongshan University, Guangzhou, Guangdong 510275, China*

[c]*Laboratory of Beijing Synchrotron Radiation, Institute of High Energy Physics, Chinese Academy of Sciences, Beijing 100039, China*

[d]*Laboratory of Excited State Processes, Changchun Institute of Optical Fine Machines and Physics, Chinese Academy of Sciences, Changchun, Jilin 130021, China*

Received 14 November 2000; accepted 7 August 2001

Abstract

The local structure and the valences of europium in $SrBPO_5$:Eu prepared in air were checked by means of XAFS at Eu–L_3 edge. From the EXAFS results, it was discovered that the doped europium atoms were nine-coordinated by oxygen atoms and the distances of bond Eu–O were 2.42 Å in the host. From the XANES data, it was found that the divalent and trivalent europium coexisted in the matrix. The emission spectra excited by VUV or UV exhibited a prominent broad band due to the $4f^6 5d–4f^7$ transition of Eu^{2+} ions, which indicated that the trivalent europium ions were reduced in air in the matrix at high temperature by the defects $[V_{Sr}]''$ formed by aliovalent substitution between Sr^{2+} and Eu^{3+} ions. The VUV excitation spectra in 100–200 nm range showed that the matrix had absorption bands with the maxima at about 130 and 150 nm, respectively.

Keywords: D. Luminescence; C. XAFS (EXAFS and XANES)

1. Introduction

By comparing the structural characteristics of a series matrixes and dopant rare earth ions, some necessary conditions for reduction of trivalent rare earth in air have been proposed [1]. These conditions are: (1) there is no oxidizing ions in matrix; (2) the doped trivalent rare earth ions must substitute aliovalent cations in host; (3) rigid three-dimensional tetrahedral network structure of anions, such as BO_4 or PO_4 exists in composite oxides matrixes; and (4) RE^{2+} have similar ionic radii to that of substituted cations. In such case, Eu^{3+}, Sm^{3+}, Yb^{3+} and Tm^{3+} could be reduced to the corresponding divalent rare earth ions in hosts such as $Ba_3(PO_4)_2$, SrB_4O_7 and SrB_6O_{10} by solid reaction at high temperature even in air [2–4].

In the silica-like network anion units BPO_4 of borophosphates, it has been suggested by Raman spectra that B and P are tetrahedral form [5,6]. Later, Kniep confirms by the crystal structural study that $SrBPO_5$ is stillwellite type [7] and contain central three single chains of BO_4 tetrahedron and link to terminal PO_4 tetrahedron to form loop-branched chains [8]. So it is expected that $SrBPO_5$ would satisfy the conditions proposed by us and it would also be a suitable matrix for the reduction of rare earth ions in air by solid state reaction at high temperature.

In recent years, the spectral properties of rare earth ions in different hosts in vacuum ultraviolet (VUV, $\lambda < 200$ nm) range have been intensively noticed. There are two reasons that compel the developments for research on rare earth ions in this VUV region. The first reason is to study the high-energy states of rare earth ions. Although the energy levels up to 50,000 cm^{-1} for most rare earth ions have been observed, the reports on $4f^n$ energy levels in VUV region are scarce. The second reason is to explore efficient VUV excited luminescent materials which could be used in mercury-free fluorescent lamps or plasma display panels. Some work has been accomplished in few hosts in the VUV range [9–13].

* Corresponding author. Tel.: +86-431-5602005; fax: +86-431-5698041.

E-mail address: suqiang@ns.ciac.jl.cn (Q. Su).

0022-3697/02/$ - see front matter
PII: S0022-3697(01)00203-7

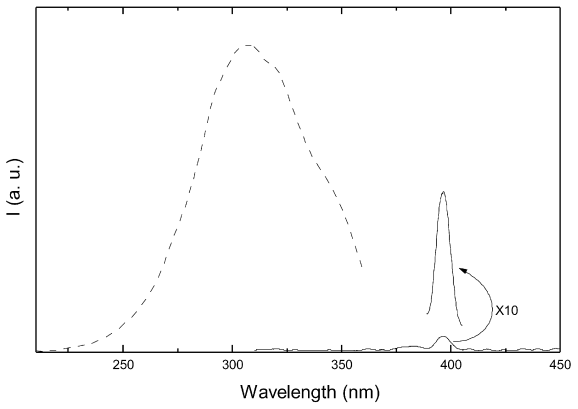

Fig. 1. Excitation spectra of Eu^{2+} (dash line, $\lambda_{em} = 388$ nm) and Eu^{3+} (solid line, $\lambda_{em} = 592$ nm) in the sample $Sr_{0.97}Eu_{0.03}BPO_5$.

In this paper, the reduced behavior of europium in $SrBPO_5$:Eu prepared in air was checked by luminescence of europium and XANES at Eu–L_3 edge. The VUV excitation spectra of the material were reported. At the same time, considering the fact that the coordination environments of luminescent centers are important for luminescent materials, the local structure of europium was determined by EXAFS at Eu–L_3 edge.

2. Experimental

The powder sample $SrBPO_5$:Eu was prepared by the method of solid phase reaction in air atmosphere. The mixed reactants, analytical-grade strontium carbonate, boric acid (excess 3 mol% to compensate the evaporation), ammonium dihydrogen phosphate and europium oxide (99.99%) were heated at 400°C for 4 h, and then fired at 1000°C for another 4 h in air atmosphere.

The structure of matrix and europium doped samples were checked by X-ray powder diffraction using CuKα_1 radiation. The XRD data indicated that all of the synthesized samples were single hexagonal phase, and were coincident with JCPDS 18-1270. The constants of matrix crystal cell calculated from observed d values were $a = 6.8692$ Å, $c = 6.7977$ Å.

The emission and UV excitation spectra were determined at room temperature and performed on a Hitachi F-4500 fluorescence spectrophotometer (resolution 0.2 nm) and a xenon lamp was used as excitation source.

The VUV excitation spectra and XAFS at Eu–L_3 edge of the sample were measured by Beijing Synchrotron Radiation Facilities (BSRF) on beam 3B1B at VUV spectral experimental station or on beam 4W1B at XAFS experimental station under normal operating conditions (2.2 GeV, 60 mA), respectively. For the determination of VUV spectra, an ARC-502 monochromator was used for excitation spectrum, an ARC-308 monochromator was used for emission spectrum and the signal was detected by an H7421-50 photomultiplier. The relative VUV excitation intensities of the samples were corrected by comparing the measured excitation intensities of the samples with the excitation intensities of sodium salicylate at the same excitation condition. For XAFS measurement, X-ray photon was defined by a slit of size $1.0(H) \times 10(V)$ mm^2 and monochromatized by a Si(111) double crystal monochromator whose energy resolution was 1.2×10^{-4} $\Delta E/E$. Because of the low contents of europium in the doped sample, the sample measurement was made in fluorescence detector and Eu_2O_3 which was used as reference sample was measured by transmission mode. All VUV and XAFS experimental data were collected at 293 K.

3. Results and discussion

3.1. The reduced behavior of europium in $SrBPO_5$:Eu prepared in air

The existence of Eu^{2+} or Eu^{3+} ions in matrixes could be probed by luminescent properties or XANES. First, it is well known that the divalent and the trivalent europium ions exhibit different luminescent transitions. Because the energy of $4f^65d$ states are usually lower than the energy of $4f^7$ states at room temperature, the divalent europium ion shows f–d transitions in the form of broad band in most matrixes; while the trivalent europium ion exhibits the f–f transitions in the form of sharp lines. Second, by XANES investigation of some rare earth compounds, it has been reported [14] that L_2 edge or L_3 edge of RE^{2+} and RE^{3+} ions locate at different peak positions, and the discrepancy is about 7.5 eV.

3.1.1. Excitation spectra

The excitation curves for Eu^{2+} and Eu^{3+} in the sample $Sr_{1-x}Eu_xBPO_5$ ($x = 0.03$) were presented in Fig. 1. The excitation spectrum of Eu^{2+} was obtained by f–d transition emission of divalent europium ion at 388 nm and the excitation spectrum of Eu^{3+} was obtained by f–f transition emission of trivalent europium ion at 592 nm, respectively. The excitation spectrum of Eu^{2+} exhibited a dominated band with a maximum at 307 nm which was caused by the permitted $4f^65d$–$4f^7(^8S_{7/2})$ transition of Eu^{2+}. And the f–f transition of Eu^{3+} led to the faint excitation band centered at 397 nm.

3.1.2. Emission spectra

The sample $Sr_{1-x}Eu_xBPO_5$ ($x = 0.03$) showed blue–violet fluorescence, as shown in Fig. 2. When the sample was excited with wavelength 307 nm, a broad emission band appeared, which was caused by $4f^7(^8S_{7/2})$ –$4f^65d$ transition of divalent europium and the maximum centered at 388 nm with half width about 33 nm. When the sample was excited with wavelength 397 nm, weak emission lines of trivalent europium could be observed, which were probably due to

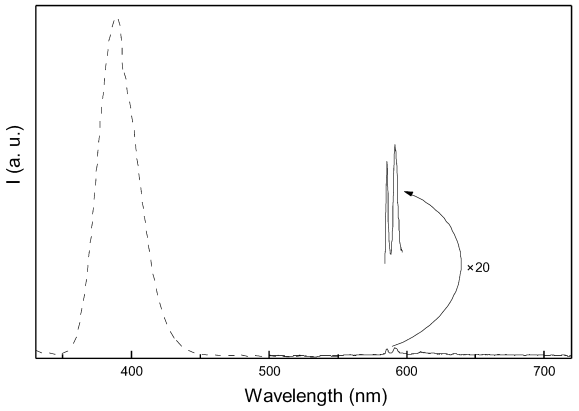

Fig. 2. Emission spectra of Eu^{2+} (dash line, $\lambda_{ex} = 307$ nm) and Eu^{3+} (solid line, $\lambda_{ex} = 397$ nm) in the sample $Sr_{0.97}Eu_{0.03}BPO_5$.

the $^5D_0$–$^7F_1$ transition of Eu^{3+} ions and were situated at 586 and 592 nm, respectively.

The luminescent spectrum of Eu^{2+} in $SrBPO_5$:Eu prepared in air is coincident with that prepared in H_2/N_2 reducing atmosphere [15]. From excitation and emission spectra, it could be observed that most of trivalent europium ions in the sample $Sr_{1-x}Eu_xBPO_5$ ($x = 0.03$) prepared in air at high temperature had been reduced to the divalent form.

3.1.3. XANES at Eu–L_3 edge

Comparing the emission intensities of divalent europium ion in samples with different doped concentration at the same condition, we found that Eu^{2+} ions showed the strongest emission when the doped concentration was 3.0 mol%. However, it was found that L_3 edge of both Eu^{2+} and Eu^{3+} obviously presented when doped concentration was 1.0 mol%. As the oscillator strength of the transition in the luminescent spectra are different for Eu^{2+} and Eu^{3+}, and it strongly affected the intensities of Eu^{2+} and Eu^{3+} emission, the Eu^{2+}/Eu^{3+} concentration ratio could be estimated from XANES. So the sample $Sr_{1-x}Eu_xBPO_5$ ($x = 0.01$) was used to perform XANES.

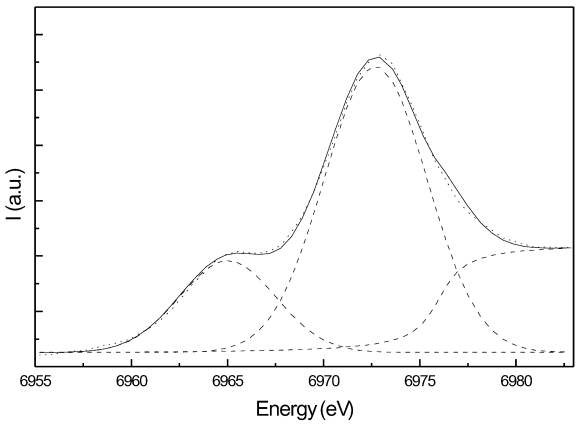

Fig. 3. XANES (dot line), fitted curves (solid line) and deconvolution lines (dash line) at Eu–L_3 edge in $Sr_{0.99}Eu_{0.01}BPO_5$.

The result of XANES at Eu–L_3 edge in $Sr_{1-x}Eu_xBPO_5$ ($x = 0.01$) is shown in Fig. 3. Fitted curve and deconvolution lines were also depicted. Double peaks appeared in XANES of the sample at Eu–L_3 edge. The lower energy edge was corresponding to Eu^{2+} ions, while the higher one was corresponding to Eu^{3+} ions. The positions of L_3 edge of Eu^{3+} and Eu^{2+} ions were at 6972.9 and 6964.9 eV, respectively. The energy of L_3 edge of Eu^{2+} was 8.0 eV lower than that of Eu^{3+}. Just as the luminescent results, the XANES results also indicated that Eu^{3+} ions could be reduced into divalent Eu^{2+} in $Sr_{1-x}Eu_xBPO_5$ ($x = 0.01$) prepared in air.

We think the mechanism of this abnormal reduction of Eu^{3+} in $Sr_{1-x}Eu_xBPO_5$ in oxygenating atmosphere is connected for two reasons. First, aliovalent substitution brings about reduction; and second, the rigid tetrahedron structure of anions AO_4 (A = B, P) guarantees the reduced valence state steadiness.

When Eu^{3+} cations were built into the matrix, they would first replace the Sr^{2+} cations. In order to keep the electroneutrality of the compound, two Eu^{3+} ions would substitute for three Sr^{2+} ions. Therefore, two positive defects of $[Eu_{Sr}]^{\cdot}$ and one negative Sr^{2+} vacancy of $[V_{Sr}]''$ would be created by each substitution. The free electrons are carried on the negative Sr^{2+} vacancy, which are produced by aliovalent substitution between doped Eu^{3+} and Sr^{2+} in host lattice. By thermally stimulated movement, the electrons on the $[V_{Sr}]''$ vacancies would be transferred to doped Eu^{3+} ions and the doped Eu^{3+} ions are reduced by these free electrons. The similar process was suggested [16] for the reduction of Eu^{3+} in $Sr_2B_5O_9Cl$:Eu by our group.

It is reported [8] that all anions are in the form of the rigid tetrahedron structure of BPO_4 in the host $SrBPO_5$, and Eu^{2+} ion (130 pm) has similar ionic radius with Sr^{2+} ion (131 pm) when they both are nine-coordinated. We think that these factors are suitable to stabilize the Eu^{2+} ions. Because the replacement easier occurred between cations which have similar ionic radii, Eu^{2+} ions occupy the substituted lattice sites of Sr^{2+} ions, the replacement can not lead to obvious distortion for tetrahedral anion BPO_4. This rigid tetrahedral structure can efficiently enclose Eu^{2+} ion, protect the inserted Eu^{2+} from the attack of the oxygen in air, so the reduced state is easy to be stabilized. The point had been supported by the facts that rare earth ions can be reduced in the matrixes such as SrB_4O_7 [1], SrB_6O_{10} [16] and BaB_8O_{13} [17]. In host SrB_4O_7 [1], all anions existed in the form of tetrahedron BO_4, the Eu^{3+} can be reduced in air. While in host BaB_8O_{13} [17], the anions are composed of triangular structure BO_3 and tetrahedron BO_4, the Eu^{3+} can also be reduced in air, but fewer Eu^{3+} ions can be reduced in BaB_8O_{13}:Eu than in SrB_4O_7:Eu [18]. And in $Sr_3B_2O_6$, $Sr_2B_2O_5$ and SrB_2O_4, the anions contain only triangular BO_3 group, Eu^{3+} ion can not be reduced in air by aliovalent substitution [1].

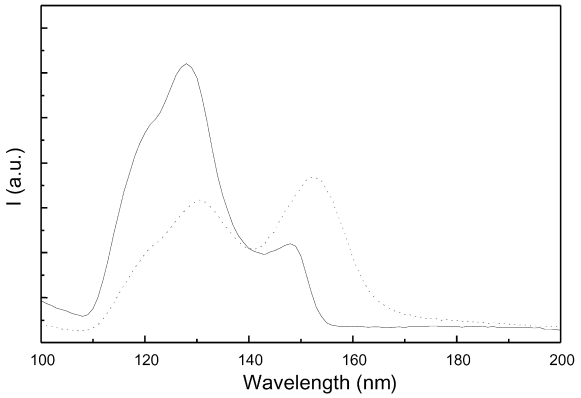

Fig. 4. VUV excitation spectra of $Sr_{0.97}Eu_{0.03}BPO_5$ (solid curve, the emission of Eu^{2+} at 398 nm was monitored; dotted curve, the emission of Eu^{3+} at 586 nm was monitored).

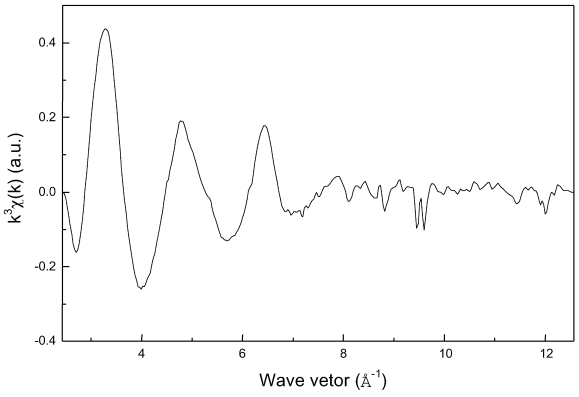

Fig. 6. Isolated k^3-weighed EXAFS oscillation of Eu–L_3 edge in $Sr_{0.90}Eu_{0.10}BPO_5$.

3.2. VUV spectra

Several mechanisms have been reported in the VUV range: (1) d–f transition of the luminescent center ions [10,11,19,20]; (2) charge transfer band (CTB) from coordination anions to luminescent center cations [10,13]; (3) f–f transition of the luminescent center ions [13]; (4) the absorption of the host lattice [10,21,22]; and (5) 4f–6s transition of the luminescent center ions [23].

Fig. 4 showed VUV excitation spectra of Eu^{2+} (solid curve) and Eu^{3+} (dash curve) emission in $Sr_{1-x}Eu_xBPO_5$ ($x = 0.03$) prepared in air, respectively. There were two bands centered around 130 (with a shoulder near 120 nm) and 150 nm in the VUV excitation spectra of both Eu^{2+} and Eu^{3+}. Because the bands were presented when monitored at either the emission of Eu^{2+} or the emission of Eu^{3+}, they were most probably caused by the absorption of the host lattice. As shown in Fig. 5, the material exhibited dominated f–d transition of Eu^{2+} at 398 nm and faint f–f transition of Eu^{3+} at 586 and 598 nm, respectively, when excited by 130 nm VUV light.

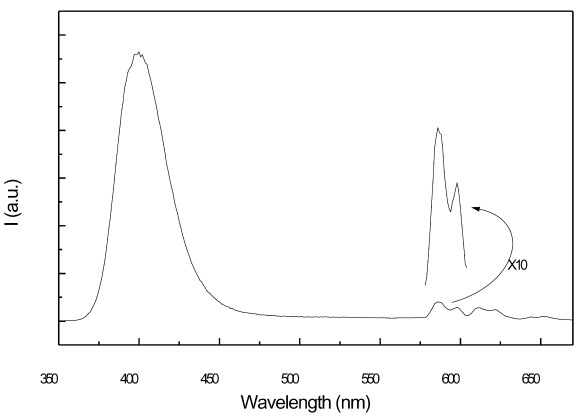

Fig. 5. 130 nm VUV excited luminescent spectra of $Sr_{0.97}Eu_{0.03}BPO_5$.

3.3. EXAFS at Eu–L_3 edge

In order to increase the accuracy of the measurement, a higher dopant sample, $Sr_{0.90}Eu_{0.10}BPO_5$ was used to perform the EXAFS at Eu–L_3 edge.

Data processing of EXAFS at Eu–L_3 edge in the samples followed standard procedures for pre-edge background subtraction and EXAFS background removal [24,25], the EXAFS χ is defined as

$$\chi(E) = [\mu(E) - \mu_0(E)]/\mu_0(E)$$

where $\mu(E)$ and $\mu_0(E)$ are the X-ray absorption coefficients for the sample and the isolated atom, respectively. The normalized EXAFS data were converted to a wave vector (k) space, using

$$k = [2m(E - E_0)/\hbar^2]^{1/2}$$

where E_0 is the maximum of the first derivative of the spectra, m is the mass of an electron, E is the photon energy, and h is Planck's constant divided by 2π. The resulting oscillations were weighed with k_3 factor and Fourier transformed, which give the radical structure function of the edge. The main peak was inversely Fourier-transformed into k space again, and was curve-fitted by the nonlinear least square curve-fitting method with the following EXAFS formula:

$$\chi(k) = \Sigma\left(N_j S/kr_j^2\right) f_j(k) \exp\left(-2\sigma_j^2 k^2\right) \sin[2kr_j + \phi_j(k)]$$

where $f_j(k)$ is the backscattering amplitude function and $\phi_j(k)$ the total phase shift function derived from reference sample Eu_2O_3, respectively. N_j is the number of atoms in the j-shell at the average distances r_j, viz. the true coordination

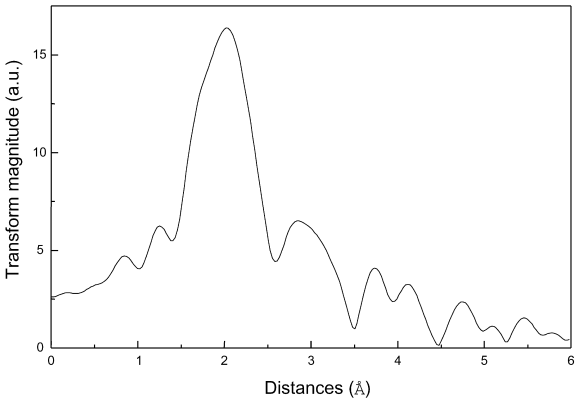

Fig. 7. Fourier transform of the k^3-weighed EXAFS spectrum of Eu–L_3 edge in $Sr_{0.90}Eu_{0.10}BPO_5$ (phase shift had not been corrected in the figure).

number of photon–electron scatters at distance r_j. S is damping factor which was fixed and evaluated also from the coordination number of the reference sample Eu_2O_3, and σ_j^2, the Debye–Waller factor, represents the variance at the distance r_j and Waller factor contains the contribution from both static disorder and thermally induced vibration displacements within a shell of neighbors.

The isolated and k^3-weighed EXAFS oscillation are shown in Figs. 6 and 7, respectively. From the EXAFS data, it could be calculated that the coordination numbers of doped europium atoms are 9 (calculated value is 9.00) the average bond distances of Eu–O are 2.42 Å and $\sigma_j^2 = 0.0007$. Obviously, from the results, it could be affirmed that the europium atoms had entered the lattice sites of subsititued strontium atoms in mixed valence configuration (Eu^{2+} and Eu^{3+}) in the matrix.

Generally consideration, the doped rare earth cations (luminescent centers) should enter the lattice sites of substituted host cations. For example, according to the structure [26,27] of SrB_4O_7, the site symmetry of Sr^{2+} was C_s, and the luminescence [28] of Sm^{2+} in SrB_4O_7:Sm^{2+} showed that doped Sm^{2+} ions also occupied the C_s sites, which implied that Sm^{2+} ions entered the substituted Sr^{2+} sites. The rare earth ions can be used as luminescent structural probe. The coordination environments of rare earth ions reflected that of substituted host cations. Besides, from the results of luminescent spectra and crystal structure, it had been reported [29,30] that EuB_4O_7, $Sr_{1-x}Eu_xB_4O_7$ and SrB_4O_7 have iso-structure.

Because the coordination structure of cations in $SrBPO_5$ had not ever been depicted, according to the above result that the europium atoms occupy the lattice site of the substituted strontium atoms in $SrBPO_5$:Eu, the coordination environments of alkaline earth ions can be determined by means of rare earth ions. The nine-coordinated strontium in $SrBPO_5$ can be deduced.

4. Conclusions

The UV–VUV excitation spectra, the UV–VUV excited luminescent spectra and XAFS (EXAFS and XANES) had been determined for luminescent material $SrBPO_5$:Eu prepared in air by solid state reaction at high temperature.

Both luminescence and XANES suggest the Eu^{3+} could be reduced to Eu^{2+} in air at high temperature. (1) In the UV excitation spectrum and the UV–VUV excited emission spectra, the characteristic d–f transition band of Eu^{2+} are presented, which implied that the trivalent europium ions were reduced. (2) XANES at Eu–L_3 edge of the material emerged the absorption of Eu^{2+} at 6964.9 eV and Eu^{3+} at 6972.9 eV, respectively. It also indicated the existence of Eu^{2+} in the sample, which were consistent with the luminescent results. Divalent europium ions could stably exist in the matrix when synthesized in oxygenating atmosphere, which were due to aliovalent replacement, the existence of the rigid tetrahedron structure of AO_4 (A = B, P) and the Eu^{2+} had similar ionic radius with the substituted Sr^{2+} in the host.

From the VUV excitation spectra, it could be observed that the material had absorption bands with the maxima at about 130 (with a shoulder near 120 nm) and 150 nm, respectively.

It could be calculated that the coordination numbers of europium atoms were nine and the average distances of bond Eu–O were 2.42 Å in the sample from EXAFS at Eu–L_3 edge. As the europium atoms entered the lattice site of the substituted strontium atoms with similar ionic radius, the nine-coordinated strontium in $SrBPO_5$ could be deduced.

Acknowledgements

This work was supported by State Key Project of Basic Research of China, the National Natural Science Foundation of China, the Foundation of Laboratory of Beijing Synchrotron Radiation, Institute of High Energy Physics, Chinese Academy of Sciences and the Foundation of Laboratory of Excited State Processes, Changchun Institute of Optical Fine Machines and Physics, Chinese Academy of Sciences.

References

[1] Z. Pei, Q. Su, J. Zhang, J. Alloys Compds. 198 (1993) 51.
[2] I. Tale, P. Kulis, V. Kronghauz, J. Luminesc. 20 (1979) 343.
[3] J.R. Peterson, W. Xu, S. Dai, Chem. Mater. 7 (1995) 1686.
[4] Q. Zeng, Z. Pei, S. Wang, Q. Su, S. Lu, Chem. Mater. 11 (1999) 605.
[5] A. Levesseur, R. Olazcuaga, M. Kbala, M. Zahir, P. Hagenmuller, M. Couzi, Sol. State Ionics 2 (1981) 205.
[6] M. Scagliotti, M. Villa, G. Chiodelli, J. Non-Cryst. Sol. 93 (1987) 350.

[7] A.A. Voronkov, Yu.A. Pyatenko, Kristallografiva 12 (1967) 258.
[8] R. Kniep, G. Gozel, B. Eisenmann, C. Rohr, M. Asbrand, M. Kizilyalli, Angew. Chem. Int. Ed. Engl. 33 (1994) 749.
[9] J. Koike, T. Kojima, R. Toyonaga, A. Kagami, T. Hase, S. Inaho, J. Electrochem. Soc. 126 (1979) 1008.
[10] J.C. Krupa, M. Queffelec, J. Alloys Compds. 250 (1997) 287.
[11] A.M. Srivastava, D.A. Doughty, W.W. Beers, J. Electrochem. Soc. 144 (1997) L190.
[12] R.T. Wegh, H. Donker, A. Meijerink, R.J. Lamminmäki, J. Hölsä, Phy. Rev. B 56 (1997) 13841.
[13] R.T. Wegh, H. Donker, K.D. Oskam, A. Meijerink, Science 283 (1999) 663.
[14] Z. Hu, G. Kaind, G. Meyer, J. Alloys Compds. 246 (1997) 186.
[15] G. Blasse, A. Bril, J. De Vries, J. Inorg. Nucl. Chem. 31 (1969) 568.
[16] Z. Pei, Q. Zeng, Q. Su, J. Sol. Stat. Chem. 145 (1999) 212.
[17] Q. Zeng, Z. Pei, S. Wang, Q. Su, Spectroscopy Lett. 32 (1999) 895.
[18] H.B. Liang, T.D. Hu, S. Wang, Q. Zeng, Z. Pei, Q. Su, Chinese J. Chem. 18 (2000) 294.
[19] E. Sarantopoulou, A.C. Cefalas, M.A. Dubinskii, C.A. Nicolaides, R.Y. Abdulsabirov, S.L. Korableva, A.K. Naumov, V.V. Semashko, Optics Communications 107 (1994) 104.
[20] Y. Zhou, R. Shu, X. Zhang, J. Shi, Z. Han, Mater. Sci. Engineering B 68 (1999) 48.
[21] A.W. Veenis, A. Bril, Philips J. Res. 33 (1978) 124.
[22] B. Saubat, C. Fouassier, P. Hagenmuller, J.C. Bourcet, Mat. Res. Bull. 16 (1981) 193.
[23] C. Shi, J. Shi, J. Deng, Z. Han, Y. Zhou, G. Zhang, J. Electr. Related Phenomena 79 (1996) 121.
[24] C. Bonnelle, C. Mandle, Advances in X-Ray Spectroscopy, Pergamon Press, Oxford, 1982.
[25] B.K. Agarwal, Springer Series in Optical Science Vol.15: X-Ray Spectroscopy, An Introduction, 2nd ed, Springer Verlag, Berlin, 1991.
[26] J. Krogh-Moe, Acta. Chem. Scand. 18 (1964) 2005.
[27] A. Perloff, S. Block, Acta Cryst. 20 (1966) 274.
[28] Q. Zeng, Z. Pei, S. Wang, Q. Su, S. Lu, J. Phys. Chem. Solids 60 (1999) 515.
[29] K. Machida, H. Hata, K. Okuno, G. Adachi, J. Shiokawa, J. Inorg. Nucl. Chem. 41 (1979) 1425.
[30] K. Machida, G. Adachi, J. Shiokawa. J. Lumin. 21 (1979) 101.